1

FLOW OVER FLAT UNIFORM TERRAIN

We start with the simplest of boundary layers, that over an infinite flat surface. Here we can assume the flow to be horizontally homogeneous. Its statistical properties are independent of horizontal position; they vary only with height and time. This assumption of *horizontal homogeneity* is essential in a first approach to understanding a process already complicated by such factors as the earth's rotation, diurnal and spatial variations in surface heating, changing weather conditions, and the coexistence of convective and shear-generated turbulence. It allows us to ignore partial derivatives of mean quantities along the horizontal axes (the advection terms) in the governing equations. Only ocean surfaces come close to the idealized infinite surface. Over land we settle for surfaces that are locally homogeneous, flat plains with short uniform vegetation, where the advection terms are small enough to be negligible.

If, in addition to horizontal homogeneity, we can assume *stationarity*, that the statistical properties of the flow do not change with time, the time derivatives in the governing equations vanish as well. This condition cannot be realized in its strict sense because of the long-term variabilities in the atmosphere. But for most applications we can treat the process as a sequence of steady states. The major simplification it permits is the introduction of time averages that represent the properties of the process and not those of the averaging time.

These two conditions clear the way for us to apply fluid dynamical theories and empirical laws developed from wind tunnel studies to the atmosphere's boundary layer. We can see why micrometeorologists in the 1950s and 1960s scoured the countryside for flat uniform sites. The experiments over the plains of Nebraska, Kansas, and Minnesota (USA), Kerang and Hay (Australia), and Tsimliansk (USSR) gave us the first inklings of universal behavior in boundary layer turbulence.

1.1 Boundary layer structure and depth

Our concept of the atmospheric boundary layer (ABL) and its vertical extent has changed significantly over the last few decades. Sutton (1953) separated the boundary layer into two regions:

1. A *surface layer* region 50–100 m deep of approximately constant (in the vertical) shearing stress, where the flow is insensitive to the earth's rotation and the wind structure is determined primarily by surface friction and the vertical gradient of temperature
2. A region above that layer extending to a height of 500–1000 m, where the shearing stress is variable and the wind structure is influenced by surface friction, temperature gradient, and the earth's rotation

The two-layer concept roughly parallels that of the inner and outer regions in laboratory shear flows, although the true extent of the similarity in the scaling laws in each of those regions to laboratory flow was not known at that time. (Velocity fluctuations scale with distance from the surface in the inner layer and with the thickness of the whole boundary layer in the outer layer.) Above these two layers is the free atmosphere, where the flow is in near-geostrophic balance and no longer influenced by surface friction.

Viewed as the height at which the wind first attains geostrophic balance, the ABL depth z_h can be expressed as (Sutton, 1953)

$$z_h = \pi \left(\frac{2K_m}{f} \right)^{1/2}, \tag{1.1}$$

where K_m is the exchange coefficient for momentum (discussed in later sections) and f is the Coriolis parameter representing the effect of the earth's rotation. f is equal to $2\pi\Omega \sin\phi, \Omega$ being the earth's rotation rate and ϕ the latitude. This definition was based on the assumption that K_m is constant with height, an unfeasible assumption, and was soon abandoned.

Theoretical considerations (Tennekes, 1982) pointed to a boundary layer depth that is proportional to u_*/f, where u_* is the friction velocity (also discussed later) representing the wind stress at the surface

$$z_h = C \left(\frac{u_*}{f} \right), \tag{1.2}$$

where C is an empirical constant. A value of $C = 0.25$ yields boundary layer heights close to observed daytime heights. In reality, the frictional and Coriolis effects are often overwhelmed by external factors such as subsidence and lapse rate evolution, so u_*/f cannot be depended on to provide reliable estimates of z_h.

Both of the above definitions assume a neutrally stable boundary layer, one in which air parcels displaced up and down adiabatically maintain exactly the

yer (ABL) and its vertical extent
cades. Sutton (1953) separated the

ep of approximately constant (in
e flow is insensitive to the earth's
mined primarily by surface friction
e
a height of 500–1000 m, where the
d structure is influenced by surface
earth's rotation

hat of the inner and outer regions in
of the similarity in the scaling laws
s not known at that time. (Velocity
ace in the inner layer and with the
uter layer.) Above these two layers
r-geostrophic balance and no longer

irst attains geostrophic balance, the
53)

$$\Big)^{1/2}, \qquad (1.1)$$

mentum (discussed in later sections)
the effect of the earth's rotation. f
tation rate and ϕ the latitude. This
t K_m is constant with height, an
ed.
982) pointed to a boundary layer
the friction velocity (also discussed
ce

$$\Big). \qquad (1.2)$$

f $C = 0.25$ yields boundary layer
n reality, the frictional and Coriolis
ctors such as subsidence and lapse
n to provide reliable estimates of z_h.
neutrally stable boundary layer, one
adiabatically maintain exactly the

same density as the surrounding air and thus experience no net buoyancy forces. The temperature stratification that produces this state, referred to in meteorology as the adiabatic lapse rate ($\simeq 1°C/100$ m drop in temperature with height), is often transitory. The more persistent states are the daytime convectively mixed boundary layer, where the temperature drops more rapidly with height than the adiabatic rate in the lower regions of the layer and displaced parcels accelerate vertically away from their original positions, and the nighttime stable boundary layer, where the temperature drops less rapidly with height and displaced parcels return to their original positions. The upper limits for these two states define the depths of the daytime and nighttime boundary layers. They are represented by

$$z_h = \begin{cases} z_i & (daytime) \\ h & (nighttime) \end{cases}, \qquad (1.3)$$

where z_i is the height of the base of the inversion layer capping the daytime boundary layer, and h is the height of the top of the nighttime ground-based turbulent layer identified in different studies as the top of the surface inversion, as the level of the wind speed maximum that develops sometimes within and sometimes above the inversion, or simply as the top of the strongest near-surface echo layer in sodar (see Chapter 6) records.

In the convective boundary layer (CBL), the capping inversion acts as a lid damping out vertical motions. The steepest gradients in the mean wind speed, wind direction, and temperature occur in the first 10% or so of the CBL; in the upper 90% of the CBL strong convective mixing smoothes out almost all vertical variations in the mean profiles (Fig. 1.1). At height z_i, the mean profiles begin

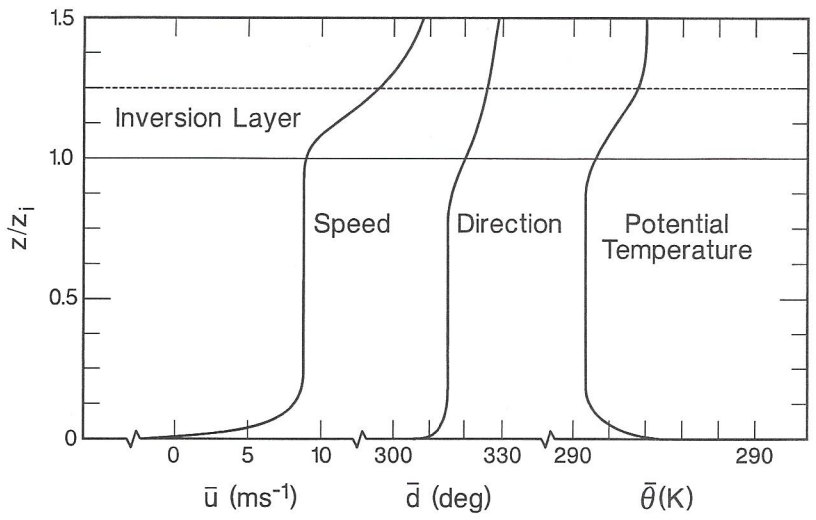

FIG. 1.1. Mean vertical profiles of wind speed, wind direction, and potential temperature in the convective boundary layer.

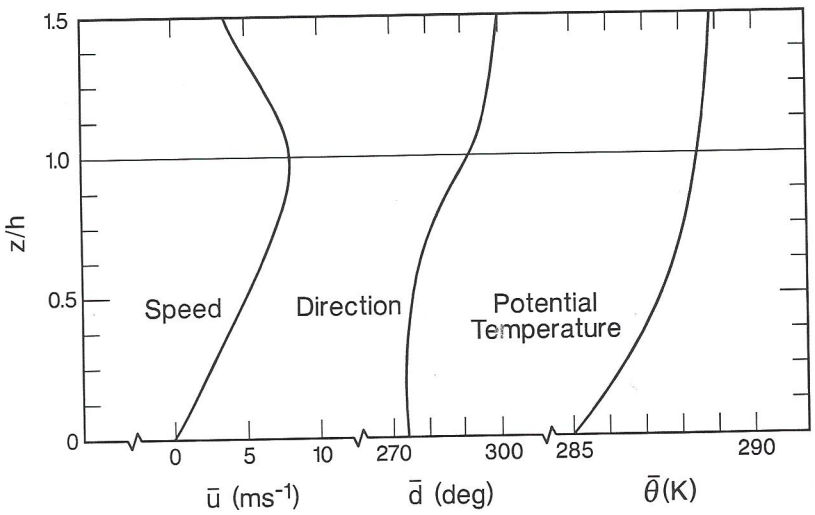

FIG. 1.2. Mean vertical profiles of wind speed, wind direction, and potential temperature in the stable boundary layer.

to depart from their near-constant CBL values to approach the free atmosphere values above.

The top of the stable boundary layer (SBL) is not as sharply defined as the top of the CBL. Turbulence levels decrease gradually with height, damped out by a combination of static stability and diminished wind shear. Although there is general agreement that h should be the height where turbulence drops to negligible levels, say 5% of surface values, its correspondence to the height of the surface inversion and/or that of the wind maximum depends very much on the history of the SBL evolution. All these significant features are represented in the wind and temperature profiles of Fig. 1.2 without the stipulation that the inversion top and the wind maximum simultaneously coincide with h. The wind maximum may be above or below the inversion top, but the sodar echoes usually stop at the lower of the two. (There is no temperature turbulence at the wind maximum and therefore no echoes from that height.) This height is probably the best estimate of h we can obtain in the absence of direct turbulence measurements.

In both Figs. 1.1 and 1.2 we have plotted temperature in the form of potential temperature θ, the temperature an air parcel with absolute temperature T and pressure p would have if brought adiabatically to the pressure at the 1000-mb (millibar) level. To the first order we can write $\theta = T + (g/c_p)\Delta z$, where g is the acceleration due to gravity, c_p is the specific heat at constant pressure, and Δz is the height difference from the 1000-mb level.

We then have

$$\frac{\partial \theta}{\partial z} = \left(\frac{\partial T}{\partial z} + \frac{g}{c_p} \right). \tag{1.4}$$

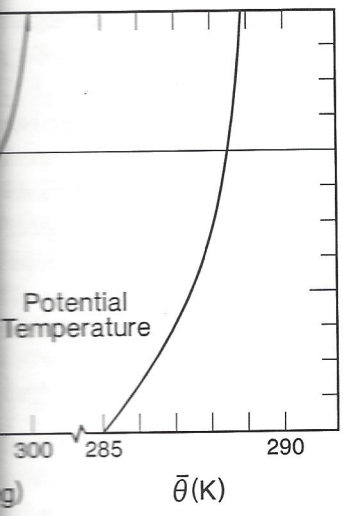

ind direction, and potential temperature

es to approach the free atmosphere

BL) is not as sharply defined as the
gradually with height, damped out
nished wind shear. Although there is
where turbulence drops to negligible
ondence to the height of the surface
depends very much on the history of
ures are represented in the wind and
stipulation that the inversion top and
with h. The wind maximum may be
ar echoes usually stop at the lower of
at the wind maximum and therefore
obably the best estimate of h we can
easurements.
d temperature in the form of potential
el with absolute temperature T and
ally to the pressure at the 1000-mb
e $\theta = T + (g/c_p)\Delta z$, where g is the
heat at constant pressure, and Δz is
L.

$$+ \frac{g}{c_p}\Big). \qquad (1.4)$$

g/c_p is the adiabatic lapse rate mentioned earlier. At 1000 mb, T and θ are, by definition, equal. In neutrally stratified air, $\partial\theta/\partial z = 0$; unstable and stable layers are easily recognized in this representation by their respectively negative $(\partial\theta/\partial z < 0)$ and positive $(\partial\theta/\partial z > 0)$ slopes.

When significant moisture is present, such as over water surfaces or in plant canopies, the contribution of moisture to the air density is included by defining a potential virtual temperature

$$\theta_v \equiv \left(\frac{\theta}{T}\right) T_v, \qquad (1.5)$$

where $T_v = T(1 + 0.61q)$. T_v, the virtual temperature, is the temperature at which dry air has the same density as moist air at the same pressure and q is the specific humidity. Over land the difference between θ and θ_v is small and often ignored. We follow the same practice here, recognizing that wherever buoyancy effects are involved, θ_v would replace θ.

1.2 States of the ABL

Although the overland ABL is evolving continuously in response to the heating and cooling of the earth's surface, it does have distinct states (Figs. 1.1 and 1.2) that can be described in fairly simple terms. Following sunrise, a convective layer develops near the ground (Fig. 1.3) as the sun's rays heat the surface and, indirectly, the air in contact with it. The convective layer grows through the morning, reaching

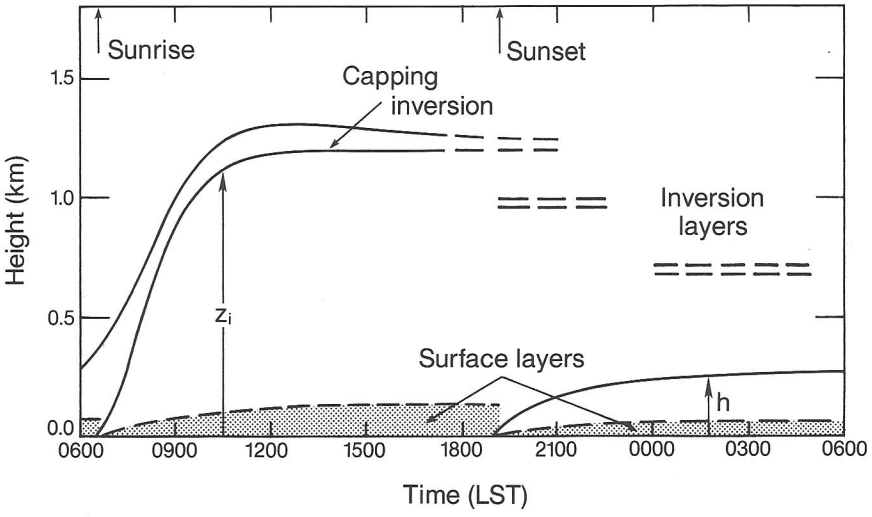

FIG. 1.3. Evolution of the convective and stable boundary layers in response to surface heating and cooling. The time indicated is Local Standard Time (LST).

heights of 1–2 km by midafternoon. The surface inversion that prevailed before sunrise evolves as the capping layer, rising with the convective layer as it grows upward. Often, the capping inversion will stay at about the same height through much of the afternoon, its strength and persistence determined largely by prior lapse rate history. A strong morning inversion followed by subsidence through the day invariably produces a well-defined capping inversion. Close to the ground, an unstable surface layer approximating Sutton's (1953) definition is clearly in evidence during the day, as seen in Fig. 1.3.

Within the CBL, convection is carried out by small plumes that merge into larger plumes (thermals) that transport the heat all the way to the capping inversion base, as depicted in Fig. 1.4. The figure also shows the entrainment process by which air from above the inversion base is drawn into the CBL in the regions of sinking motion. Occasionally, the more energetic thermals penetrate the capping inversion, but for the most part, they simply distort the upper interface of the CBL, making it appear highly convoluted. Horizontal roll vortices and dust devils also appear when conditions favor their development, adding to the modes available for convective mixing in the CBL.

With the approach of sunset, the capping inversion weakens and becomes patchy as one or more shallow inversion layers form below it (Fig. 1.5). At this time there is a rapid collapse of turbulent motions in the boundary layer as the buoyant plumes that maintain them lose their energy source near the surface where the ground is cooling quickly from radiative heat loss to space. The air immediately above the surface cools and mixes progressively upward through the action of turbulence generated by wind shear. The inversion that begins to form at the surface grows steadily to a depth of 100–200 m by midnight. A shallow, stable

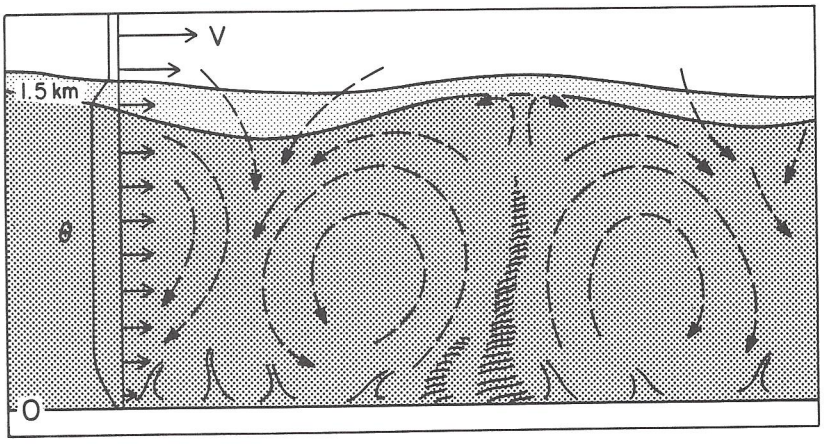

Fig. 1.4. Schematic of convective boundary layer circulation and entrainment of air through the capping inversion (from Wyngaard, 1990).

face inversion that prevailed before
ith the convective layer as it grows
y at about the same height through
istence determined largely by prior
followed by subsidence through the
ing inversion. Close to the ground,
ton's (1953) definition is clearly in

ut by small plumes that merge into
t all the way to the capping inversion
shows the entrainment process by
rawn into the CBL in the regions of
getic thermals penetrate the capping
istort the upper interface of the CBL,
tal roll vortices and dust devils also
nent, adding to the modes available

ng inversion weakens and becomes
ers form below it (Fig. 1.5). At this
notions in the boundary layer as the
eir energy source near the surface
adiative heat loss to space. The air
es progressively upward through the
. The inversion that begins to form at
200 m by midnight. A shallow, stable

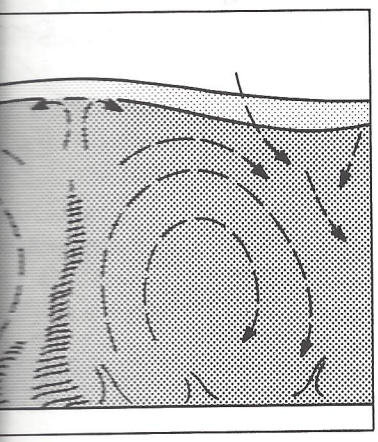

circulation and entrainment of air through

surface layer can be discerned here as well (Fig. 1.3), where the flow remains sensitive to the presence of the boundary below. Flow within the SBL is characterized by strong wind shear, small eddies, and occasional wave activity (Fig. 1.5); stratified inversion layers may appear and disappear above the SBL. The wind maximum (or low-level jet, as it is often called) may develop within the inversion or above it, as mentioned earlier. Gravity-driven drainage winds usually have their maxima within the inversion layer, but jets that form in response to the inertial oscillations induced by the earth's rotation develop considerably above the surface inversion and move downward as the night progresses.

The SBL seldom, if ever, attains the same state of equilibrium reached by the CBL. The mean wind and temperature profiles continue to evolve through the night and even small slopes in the terrain generate drainage winds. Internal gravity waves may grow and propagate. Usually by sunrise, these disturbances settle down and the stage is set for the development of a new CBL.

This sequence of CBL and SBL evolution is typical for land surfaces in the midlatitudes. In the tropics, the base of the trade wind inversion ($\sim$ 1.5 km) serves as the upper boundary for all vertical transfers, including (almost always) cumulus convection. When clouds are present, the subcloud layer (which extends about 100 m below the cloud base) acts much like the capping inversion in Fig. 1.1. The base of this subcloud layer ($\sim$ 600 m), where θ_v begins to increase to its cloud base values, is taken as the boundary layer top and used as the scaling height for the convection processes below (LeMone, 1978). Over oceans within the tropics, temperature gradients tend to be very close to the adiabatic value, and convection is supported mainly by latent heat from moisture flux at the surface. Nevertheless, the marine CBLs show surprising similarities to CBLs over land (LeMone, 1978).

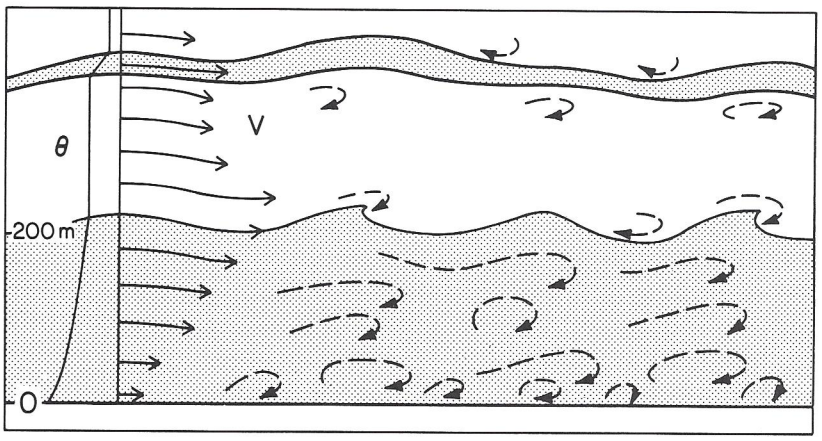

FIG. 1.5. Schematic of stable boundary layer flow showing eddy structure, waves, and elevated inversion layer (from Wyngaard, 1990).

LAYER FLOWS

ns of horizontal homogeneity and
urface layer than elsewhere in the
al gradients controlling the transfer
ey raise the possibility that simple
r diffusion in laminar flows, might
tical fluxes of these properties and
ceived by investigators in the 1950s
eorology. Our perception is broader
d analyzed over the years did yield
se as a baseline for testing surface

usion to turbulent transport in the
entum (τ), heat (H), and moisture
ion z:

(1.6)

$\frac{\partial \overline{\theta}}{\partial z}$, (1.7)

$\frac{\overline{q}}{z}$, (1.8)

change coefficients for momentum,
streamwise wind component, mean
midity; and ρ is the density of air.
fined positive downward.) The ex-
scosity, conductivity, and diffusivity
ally three orders of magnitude larger.
change in the atmosphere is known

s dimensions of stress (force/area).
and τ_y. In the surface layer over
ght is small enough to be negligible.
the wind direction with height, and
ort as a one-dimensional problem in
geneous, we can assume that $\overline{u}$, like
al. Aligning the x direction with the
in the surface layer.
known as the friction velocity, to
ground,

$$\tau_0 = \rho u_*^2.$$

This velocity, which varies with the nature of the surface and the magnitude of the wind, has emerged as an important scaling parameter in surface layer studies.

1.3.2 *Logarithmic wind profile*

The introduction of u_* leads to a simple formulation for wind profiles in a neutrally stratified atmosphere. We can represent K_m, which has dimensions of length $\times$ velocity, as the product of the two surface layer scaling parameters with those dimensions, height z and u_*:

$$K_m = k\, u_*\, z, \tag{1.9}$$

where k is the constant of proportionality. Substituting for τ and K_m in (1.6), we get

$$\frac{\partial \overline{u}}{\partial z} = \frac{u_*}{kz}. \tag{1.10}$$

Integration of (1.10) yields the classical logarithmic wind profile

$$\overline{u}(z) = \frac{u_*}{k} \ln\left(\frac{z}{z_0}\right). \tag{1.11}$$

Here z_0, the constant of integration (known as the roughness length), is the height at which $\overline{u}$, extrapolated downward, vanishes. Laboratory measurements indicate z_0 to be approximately 1/30 the height of the roughness elements, but over natural flat terrain the factor is often observed to be larger (Yaglom, 1979). The constant k is known as the von Karman constant, with reported values ranging from 0.35 to 0.43. For this constant we adopt a value of 0.4, the one most generally accepted in boundary layer work today.

The logarithmic wind profile is strictly valid only for the neutral atmosphere. As the atmosphere becomes more stable or unstable, the profile departs from being logarithmic (Fig. 1.6). For most applications very close to the ground (i.e., $z < 10$ m), however, the wind profile can be assumed to be almost always logarithmic. This allows us to use the relationships in (1.6), (1.7), and (1.8) to compute the fluxes from gradient measurement of properties in the layer.

Thus, if $\overline{u}_1$ and $\overline{u}_2$ are the mean winds measured at two heights z_1 and z_2, we have

$$\overline{u}_2 - \overline{u}_1 = \frac{u_*}{k} \ln\left(\frac{z_2}{z_1}\right). \tag{1.12}$$

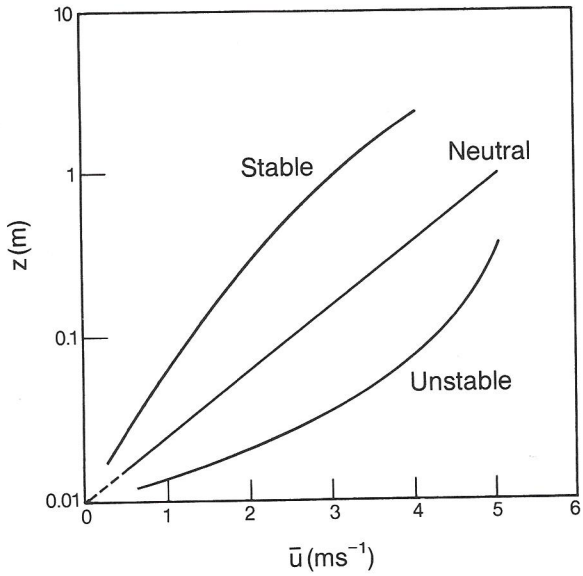

FIG. 1.6. Wind profile in stable, neutral, and unstable air.

We can now write

$$K_m = kz_r\, u_* = \frac{k^2 z_r}{\ln(z_2/z_1)}(\overline{u}_2 - \overline{u}_1), \tag{1.13}$$

substituting for u_* from (1.12). If the reference height z_r is the geometric mean of z_1 and z_2, that is, $(z_1 z_2)^{1/2}$, then at $z = z_r$, the mean wind speed is equal to $(\overline{u}_1 + \overline{u}_2)/2$.

Now, if we assume that close to the ground $K_m = K_h = K_q$ (Panofsky and Dutton, 1984), all we need for computing the vertical fluxes are the mean values of θ and q measured at the same heights at which $\overline{u}_1$ and $\overline{u}_2$ are observed. If we can also assume that their profiles are approximately logarithmic, we can, using (1.10) and (1.12), express the gradient of the mean of any such variable ζ as

$$\frac{\partial \overline{\zeta}}{\partial z} \simeq \frac{\overline{\zeta}_2 - \overline{\zeta}_1}{z_r \ln(z_2/z_1)}. \tag{1.14}$$

The fluxes of momentum, heat, and moisture assume the form

$$\frac{\tau}{\rho} = \left(\frac{k}{\ln(z_2/z_1)}\right)^2 (\overline{u}_2 - \overline{u}_1)^2, \tag{1.15}$$

$$\frac{H}{\rho c_p} = -\left(\frac{k}{\ln(z_2/z_1)}\right)^2 (\overline{u}_2 - \overline{u}_1)(\overline{\theta}_2 - \overline{\theta}_1), \tag{1.16}$$

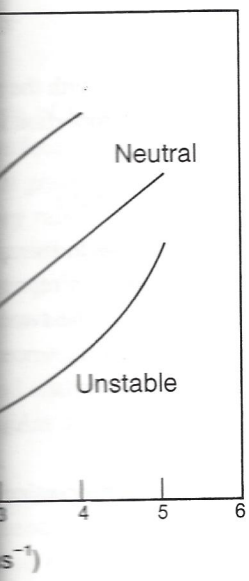

s^{-1})

neutral, and unstable air.

$$\frac{z_r}{z_1)}(\overline{u}_2 - \overline{u}_1), \tag{1.13}$$

ence height z_r is the geometric mean
z_r, the mean wind speed is equal to

ound $K_m = K_h = K_q$ (Panofsky and
he vertical fluxes are the mean values
which $\overline{u}_1$ and $\overline{u}_2$ are observed. If we
oximately logarithmic, we can, using
e mean of any such variable ζ as

$$\frac{-\overline{\zeta}_1}{z_2/z_1)}. \tag{1.14}$$

re assume the form

$$\overline{u}_2 - \overline{u}_1)^2, \tag{1.15}$$

$$(\overline{u}_2 - \overline{u}_1)(\overline{\theta}_2 - \overline{\theta}_1), \tag{1.16}$$

$$\frac{E}{\rho} = -\left(\frac{k}{\ln(z_2/z_1)}\right)^2 (\overline{u}_2 - \overline{u}_1)(\overline{q}_2 - \overline{q}_1). \tag{1.17}$$

Estimation of fluxes from profiles is subject to several constraints. We require the fluxes to be constant with height, which implies uniform flat terrain and observing heights well within the surface layer. The logarithmic law applies strictly to neutral surface layers; the estimates become less reliable as the stability departs from neutral and the profiles deviate more and more from logarithmic.

1.3.3 *Eddy correlation and fluxes*

Earlier in this chapter we defined the fluxes of momentum, heat, and moisture in terms of the mean vertical gradients of those properties. Because these fluxes are almost entirely the result of turbulent mixing, we should be able to define them more directly in terms of the turbulent (or eddy) components of velocities and of the properties being transferred. Mean flux across any plane implies correlation between the wind component normal to that plane and the entity in question. In the covariance between the two, we have a direct measure of the flux across the plane.

We start with the definition of velocity components u, v, and w along right-handed coordinate axes x, y, and z, respectively. These velocities and scalars such as θ and q can each be separated into a mean component denoted by an overbar and an eddy component denoted by a prime:

$$\begin{aligned} u &= \overline{u} + u' \\ v &= \overline{v} + v' \\ w &= \overline{w} + w' \\ \theta &= \overline{\theta} + \theta' \\ q &= \overline{q} + q'. \end{aligned}$$

By definition, we have $\overline{u'} = \overline{v'} = \overline{w'} = \overline{\theta'} = \overline{q'} = 0$. If the x axis is defined in the direction of the mean flow, $\overline{v} = \overline{w} = 0$; only $\overline{u} \neq 0$. Over a flat, level, homogeneous surface, we take x and y to be horizontal and z to be vertical and positive upwards.

The fluxes can now be written as

$$\tau = -\rho\overline{u'w'} \tag{1.18}$$

$$H = \rho c_p \overline{w'\theta'} \tag{1.19}$$

$$E = \rho\overline{w'q'}. \tag{1.20}$$

The covariance terms on the right are unambiguous measures of the fluxes, requiring no assumptions about the mixing properties of turbulence. To realize them,

however, we need fast-response sensors that can faithfully follow the fluctuations in all the variables and digital sampling at rates (10–20 Hz depending on height), much faster than needed for mean profile measurements. (The mean products of the velocity fluctuations are referred to, in general, as Reynolds stresses, and $-\rho\overline{u'w'}$, in particular, as the Reynolds shear stress.)

1.3.4 *Measures of stability*

We have seen how the ABL responds to changes in stability brought about by the heating and cooling of the ground. As we search for universal behavior in the boundary layer, we need to establish a proper measure of stability in the surface layer. The most widely used indicator of stability in laboratory and early atmospheric work is the gradient Richardson number Ri, a nondimensional parameter representing the relative importance of buoyancy and shear in producing turbulence:

$$Ri = \frac{(g/\overline{\theta})(\partial\overline{\theta}/\partial z)}{(\partial\overline{u}/\partial z)^2}, \tag{1.21}$$

where g is the acceleration due to gravity (the term $g/\overline{\theta}$ is referred to as the buoyancy parameter[1]). The advantage in using the Richardson number is that it contains gradients of mean quantities that are easy to measure. Ri is positive for stable stratification, negative for unstable stratification, and zero for neutral stratification. Above a critical value Ri_c ($= 0.25$ for inviscid flow), the flow undergoes a transition from turbulent flow to laminar. Between values 0 and Ri_c, turbulence is almost entirely mechanical in origin, generated by wind shear; at $Ri < 0$, we have a mixture of both mechanical and convective turbulence. The disadvantage in using Ri is that it is an unknown function of height and therefore not an appropriate stability parameter for characterizing surface layer structure.

Two other forms of the Richardson number, R_f the flux Richardson number and R_b the bulk Richardson number, are sometimes used. R_f is the ratio of the rate of production of turbulence by buoyancy to that by shear:

$$R_f = \frac{(g/\overline{\theta})\overline{w'\theta'}}{\overline{u'w'}(\partial\,\overline{u}/\partial z)} \simeq \frac{K_h}{K_m}\,Ri. \tag{1.22}$$

In (1.22) the numerator represents the production (or destruction) of turbulence by thermal stratification, and the denominator represents the production by turbulent stress working against the mean strain. We will be discussing these concepts

[1] Strictly speaking, the buoyancy parameter $g/\overline{\theta}$ should be $g/T_r(z)$, where $T_r(z)$ is a hydrostatic adiabatic reference state defined by $\partial T_r/\partial z = -g/c_p$ and $T_r(z_r) = \overline{T}(z_r)$ (z_r being the reference height). For practical purposes, in the ABL we can write $g/T_r(z_r) \simeq g/\overline{T}(z) \simeq g/\overline{\theta}(z)$.

later in the context of the turbulent kinetic energy budget in the surface layer. Although R_f properly characterizes the effect of flow stratification on turbulence, it is awkward to use in practice, being a mixture of eddy correlations and mean gradients, and is therefore seldom used.

R_b is a useful indicator of stability close to the ground, particularly under conditions of low wind shear when Ri becomes undependable:

$$R_b = \frac{(g/\overline{\theta})(\overline{\theta}_z - \overline{\theta}_0)/2}{(\overline{u}_z/z)^2}, \tag{1.23}$$

where $\overline{\theta}_z$ and $\overline{\theta}_0$ denote mean potential temperatures at height z and the surface, respectively, and $\overline{u}_z$ denotes the mean wind at height z. In light winds, the denominator in this expression behaves more predictably than in (1.21). Its application is limited because it is only a crude approximation of Ri and requires nomograms (Panofsky and Dutton, 1984) relating it to Ri and $\ln(z/z_0)$ to render it useful.

The stability parameter now recognized by boundary layer meteorologists as appropriate for the surface layer is the ratio of height z to the scaling length L (the Obukhov length), which can be expressed as

$$\frac{z}{L} = -\frac{(g/\overline{\theta})(\overline{w'\theta'})_0}{u_*^3/kz} \tag{1.24}$$

where $(\overline{w'\theta'})_0$ denotes temperature flux at the surface. The ratio z/L is essentially the same as R_f with substitutions in the denominator of u_*/kz for $\partial u/\partial z$ and u_*^2 for $-(\overline{u'w'})$. The negative sign is introduced so z/L has the same sign as Ri and R_f, negative when the atmosphere is unstable and positive when it is stable. This quantity is more useful than Ri because L can be assumed constant through the surface layer. It also implies that within the surface layer [where this parameter forms the basis for the similarity hypothesis proposed by Monin and Obukhov (1954)], the effects of varying height and stability (as represented by L) are interchangeable.

1.3.5 *Monin-Obukhov similarity*

Empirical evidence from field experiments conducted over flat terrain points to a surface layer where the structure of turbulence is determined by a few key parameters as proposed by Monin and Obukhov (1954). These are the height z, the buoyancy parameter $g/\overline{\theta}$, the kinematic surface stress τ_0/ρ, and the surface temperature flux $H_0/\rho c_p$. According to the Monin-Obukhov (M-O) hypothesis, various atmospheric parameters and statistics, such as gradients, variances, and covariances, when normalized by appropriate powers of the scaling velocity u_* and the scaling temperature T_* (as defined below), become universal functions of z/L:

$$u_* = \left[-(\overline{u'w'})_0\right]^{1/2} \tag{1.25a}$$

$$T_* = \frac{-(\overline{w'\theta'})_0}{u_*}. \tag{1.25b}$$

Although defined strictly in terms of fluxes at the surface, u_* and T_* are evaluated, in practice, from measurements of the fluxes at some convenient height within the surface layer where their vertical variations can be assumed negligible with height, a reasonable assumption for $z \lesssim |L|$ (Haugen et al., 1971). The important nondimensional forms to emerge in the surface layer are

$$\phi_m = (kz/u_*)(\partial\overline{u}/\partial z) \quad \text{wind shear,} \tag{1.26}$$

$$\phi_h = (kz/T_*)(\partial\overline{\theta}/\partial z) \quad \text{thermal stratification,} \tag{1.27}$$

$$\phi_w = \sigma_w/u_* \quad \text{variability in } w, \tag{1.28}$$

$$\phi_\theta = \sigma_\theta/|T_*| \quad \text{variability in } \theta, \tag{1.29}$$

$$\phi_\epsilon = kz\epsilon/u_*^3 \quad \text{dissipation of turbulent kinetic energy,} \tag{1.30}$$

where σ_w and σ_θ are the standard deviations of w and θ, and ϵ is the rate of dissipation of turbulent kinetic energy. We introduce ϵ here because of its relevance to discussions of the turbulent kinetic energy budget later in this chapter. Its relationship to velocity spectra will be discussed in Chapter 2.

All the above functions follow M-O scaling with surprisingly small scatter, as evident in the plots of the Kansas data (Businger et al., 1971; Wyngaard and Coté, 1971). The following formulations are essentially the Kansas results, reexamined and refined through comparison with other observations (Dyer, 1974; Högström, 1988):

$$\phi_m = \begin{cases} (1+16\,|z/L|)^{-1/4}, & -2 \le z/L \le 0 \\ (1+5\,z/L), & 0 \le z/L \le 1 \end{cases} \tag{1.31}$$

$$\phi_h = \begin{cases} (1+16\,|z/L|)^{-1/2}, & -2 \le z/L \le 0 \\ (1+5\,z/L), & 0 \le z/L \le 1 \end{cases} \tag{1.32}$$

$$\phi_w = \begin{cases} 1.25(1+3\,|z/L|)^{1/3}, & -2 \le z/L \le 0 \\ 1.25(1+0.2\,z/L), & 0 \le z/L \le 1 \end{cases} \tag{1.33}$$

$$\phi_\theta = \begin{cases} 2(1+9.5\,|z/L|)^{-1/3}, & -2 \le z/L \le 0 \\ 2(1+0.5\,z/L)^{-1}, & 0 \le z/L \le 1 \end{cases} \tag{1.34}$$

$$\phi_\epsilon = \begin{cases} (1+0.5\,|z/L|^{2/3})^{3/2}, & -2 \le z/L \le 0 \\ (1+5\,z/L), & 0 \le z/L \le 1. \end{cases} \tag{1.35}$$

The forms of these functions, plotted in Fig. 1.7, cannot be predicted from dimensional analysis. They have to be determined empirically from field experiments. Conspicuously absent from this list are forms for the standard deviations

$]^{1/2}$ (1.25a)

(1.25b)

he surface, u_* and T_* are evaluated,
s at some convenient height within
ns can be assumed negligible with
Haugen et al., 1971). The important
e layer are

(1.26)

tification, (1.27)

in w, (1.28)

in θ, (1.29)

of turbulent kinetic energy, (1.30)

ns of w and θ, and ϵ is the rate of
oduce ϵ here because of its relevance
gy budget later in this chapter. Its
ssed in Chapter 2.
ing with surprisingly small scatter, as
ger et al., 1971; Wyngaard and Coté,
tially the Kansas results, reexamined
bservations (Dyer, 1974; Högström,

$$\begin{matrix} -2 \le z/L \le 0 \\ 0 \le z/L \le 1 \end{matrix} \quad (1.31)$$

$$\begin{matrix} -2 \le z/L \le 0 \\ 0 \le z/L \le 1 \end{matrix} \quad (1.32)$$

$$\begin{matrix} -2 \le z/L \le 0 \\ 0 \le z/L \le 1 \end{matrix} \quad (1.33)$$

$$\begin{matrix} -2 \le z/L \le 0 \\ 0 \le z/L \le 1 \end{matrix} \quad (1.34)$$

$$\begin{matrix} -2 \le z/L \le 0 \\ 0 \le z/L \le 1. \end{matrix} \quad (1.35)$$

in Fig. 1.7, cannot be predicted from
rmined empirically from field experi-
are forms for the standard deviations

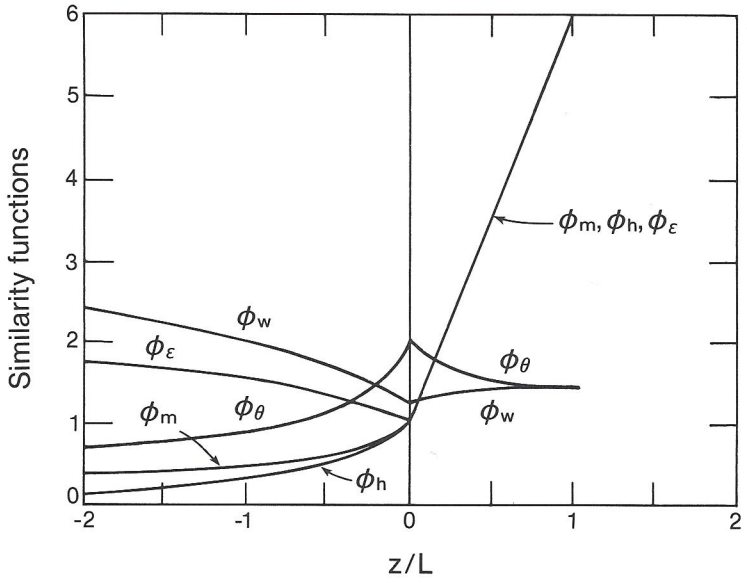

FIG. 1.7. Similarity functions in the surface layer.

of u and v. They do not follow M-O similarity for reasons that will become clear as we examine the behavior of their spectra in Chapter 2. We can, however, expect scalar properties such as q and their fluxes to follow M-O similarity and to have functional forms resembling those of ϕ_h and ϕ_θ when normalized by the appropriate scaling parameter, in this case q_*, defined as $-(\overline{w'q'})_0/u_*$.

In our idealizations of these wind profiles, we have forced $\phi_m = \phi_h = \phi_\epsilon = 1$ at $z/L = 0$. Not all experiments support the assumption of unity for neutral ϕ_m and ϕ_h (Businger et al., 1971) but many do (Dyer, 1974; Dyer and Bradley, 1982). The forms we have chosen for ϕ_m and ϕ_h are known as the Businger-Dyer relations (Businger, 1988; Panofsky and Dutton, 1984). We have ϕ_ϵ also approaching unity at neutral stability because of the expected balance between shear production and viscous dissipation of turbulence in the absence of any buoyant production and transport:

$$\begin{aligned} \epsilon &= -(\overline{u'w'})\,\frac{\partial \overline{u}}{\partial z} \\ &= u_*^2 \left(\frac{u_*}{kz}\right). \end{aligned} \quad (1.36)$$

Having chosen a form for ϕ_m, we can derive an expression for the diabatic (nonneutral) wind profile. (The mean profiles $\overline{u}/u_*, \overline{\theta}/T_*$, etc., are not functions of z/L; they have to be derived from the gradients.) Integration of ϕ_m yields a modified logarithmic profile (Panofsky and Dutton, 1984):

$$\overline{u}(z) = \frac{u_*}{k}\,[\ln(z/z_0) - \psi_m], \tag{1.37}$$

where the diabatic term ψ_m is the integral of $(1 - \phi_m)/(z/L)$ over limits $z_0/$ to z/L. ψ_m is thus a function of z/L. The expression for ψ_m is simple for th stable surface layer ($-5\ z/L$, for our choice of ϕ_m) but more cumbersome for th unstable layer. ψ_m values corresponding to ϕ_m in unstable air (1.31) are presente in Table 1.1.

The basic definitions for ϕ_m and ϕ_h in (1.26) and (1.27) lead to the followi identities:

$$K_h/K_m \equiv \phi_m/\phi_h, \tag{1.38}$$

$$Ri \equiv (z/L)(\phi_h/\phi_m^2), \tag{1.38}$$

$$R_f \equiv (z/L)/\phi_m. \tag{1.38}$$

Table 1.1. ϕ_m and ψ_m in Unstable Air

z/L	ϕ_m	ψ_m
0.00	1.000	0.000
−0.10	0.788	0.284
−0.20	0.699	0.461
−0.30	0.644	0.595
−0.40	0.606	0.702
−0.50	0.577	0.793
−0.60	0.554	0.873
−0.70	0.535	0.943
−0.80	0.519	1.006
−0.90	0.505	1.063
−1.00	0.493	1.116
−1.10	0.482	1.165
−1.20	0.472	1.211
−1.30	0.463	1.253
−1.40	0.455	1.293
−1.50	0.447	1.331
−1.60	0.440	1.367
−1.70	0.434	1.401
−1.80	0.428	1.434
−1.90	0.422	1.465
−2.00	0.417	1.495